Experimental study of the impact of carrying a telecom signal on LOCSET-based coherent beam combining

Bastien Rouzé, Pierre Pichon, Mathilde Gay, Laurent Bramerie, Laurent Lombard, Anne Durécu

Research Article | Vol. 31, No. 16 / 31 Jul 2023 / Optics Express 26552
Optics EXPRESS

Experimental study of the impact of carrying a telecom signal on LOCSET-based coherent beam combining

BASTIEN ROUZÉ,[1] PIERRE PICHON,[1,*] MATHILDE GAY,[2] LAURENT BRAMERIE,[2] LAURENT LOMBARD,[1] AND ANNE DURÉCU[1]

[1]DOTA, ONERA, Université Paris Saclay – 91120 Palaiseau, France
[2]Institut Foton, CNRS UMR 6082, Université de Rennes – 22300 Lannion, France
[*]pierre.pichon@onera.fr

Abstract: We report on what is, to our knowledge, one of the first realizations of a CBC (coherent beam combining)-based laser emitter carrying a 10.66 Gb/s telecom signal in free-space optics, within the laboratory environment. Two telecom modulations have been tested: NRZ (non-return-to-zero, in amplitude) and DPSK (differential phase-shift keying, in phase). The modulated signal is split and amplified in three fiber amplifiers, delivering up to 3 W each. CBC of data amplified signals is achieved with residual phase errors well below $< \lambda/60$ RMS, using a phase-tagging technique (LOCSET). A first analysis of the influence of various parameters (such as phase-tagging modulation depth, optical path difference, number of channels, amplifier power) on the locking and data transmission quality is investigated. The study shows that the phase-tagging modulation depth and optical path difference are the main critical issues when carrying data on a CBC signal.

1. Introduction

High-power reliable optical feeder links for satellite telecommunication are promising to go beyond the current constraints of Radio Frequency (RF) links, such as frequency coordination, bandwidth limitation, beam divergence, or even cost efficiency [1–3]. However, the development of high-throughput optical links must overcome different challenges [2–4], such as mitigation of atmospheric turbulences by ensuring wavefront control [5], or the reliability of high-power fiber laser sources, including all components from the fiber to free-space optics [6].

Coherent beam combining (CBC) at the transmitter side could be a solution to large required link power of satellite communication based on optical feeder links [7–9]. In this approach, the signal carrying data is split into several replicas that are amplified independently and coherently recombined with a fine phase adjustment in order to maximize the power density deposited on the brightest central interference lobe [10].

As of today, CBC has been demonstrated for many configurations ranging from near-field beam superimposition [11] to tiled-aperture target-in-the-loop far-field beam combination [12,13], or even far-field intensity distribution control [14,15]. Various phase-locking techniques have been designed to achieve stable combination, such as interferometric measurement [16], far-field based-metrics optimization by Stochastic Parallel Gradient Descent (SPGD) [12], or Locking of Optical Coherence via Single-detector Electronic-frequency Tagging (LOCSET) [17]. However, it has never been demonstrated experimentally that an optical field carrying data will be coherently combined with minimal performance loss, by showing simultaneously low Bit Error Rate (BER) measurements corresponding to low residual phase errors.

In this paper, we propose an experimental study of CBC with a telecom modulation. We study for the first time on the one hand the impact of the telecom signal on the quality of the far-field fringes and the residual phase, and on the other hand, the impact of the LOCSET phase-locking

#497156 https://doi.org/10.1364/OE.497156
Journal © 2023 Received 2 Jun 2023; revised 7 Jul 2023; accepted 7 Jul 2023; published 25 Jul 2023

Optics EXPRESS

algorithm on the telecom performance. Furthermore, power disparity over the fiber array has been investigated to determine if the use of such laser as an optical feeder link would be highly dependent on system maintenance to ensure low error data transfer.

2. Telecom-CBC laser emitter setups

The telecom experiments presented in this paper have been conducted on modified versions of our CBC laser developed previously [13] where the continuous single frequency local oscillator has been replaced by a telecom signal and where a telecom receiver for transmission analysis has been used for BER (bit error rate) measurement. Two configurations have been tested: an all-fiber (AF) configuration and a free-space optic (FSO) configuration. The AF configuration is a simple setup limited to a two-channels, non-amplified all-fiber configuration, used to determine the impact of the sole phase-locking amplitude tagging on the telecom signal BER without any FSO contribution. In our FSO scheme up to three amplified channels are combined allowing to test the effects of the signal amplification and power disparity of the fiber array on the BER. In the following we describe these two setups. All optical fibers mentioned are polarization maintaining. More details on other components can be found in [13].

2.1. All-fiber configuration (AF)

The AF configuration is a two channels master oscillator power amplifier (MOPA) architecture (Fig. 1). The master oscillator (MO) is a linearly polarized continuous wave laser (CW) emitting 16 mW at $\lambda = 1545$ nm. To transmit a telecom signal, the MO output is modulated by a $LiNbO_3$ Mach Zehnder Modulator (MZM) fed by a 10.66 Gb/s pseudorandom binary sequence (PRBS) with a length of $2^{31}-1$ bits. Both Non-Return-to-Zero (NRZ) and Differential-Phase-Shift-Keying (DPSK) signals can be generated in our setup by changing DC bias and peak-to-peak driving voltage on the MZM. The modulated signal is then amplified by an Erbium/Ytterbium co-doped fiber amplifier (EDFA) up to 100 mW. This EDFA is then connected to a 1-to-8 fiber splitter of which two channels are used: the reference channel and the phase-locked channel. They both include an electro-optic modulator (EOM). The reference channel EOM is not active, while the phase-locked channel EOM is tagged with a 26 MHz low-amplitude phase modulation used by LOCSET phase controller [13,17] and compensates for phase variations relative to the reference channel. Beam combination is achieved with a 90/10 coupler.

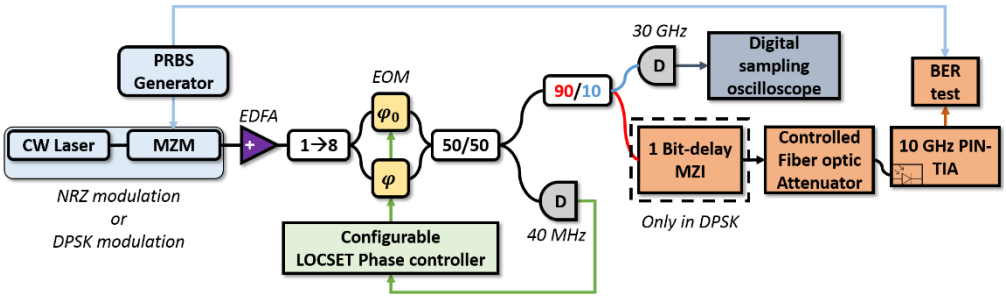

Fig. 1. The all-fiber Telecom-CBC laser emitter setup. Pseudorandom binary sequence (PRBS) is fed to the Mach-Zehnder Modulator (MZM) in order to deliver a DPSK modulated signal. This signal is amplified in an Erbium-doped fiber amplifier (EDFA) before being split towards the Electro-optical phase modulators (EOM or φ). Photodiodes (D) are used for both phase-locking and signal observation. Mach-Zehnder interferometer (MZI) allows for Bit Error Rate (BER) measurement via the PIN photodiode and its transimpedance amplifier (PIN-TIA). Similar layout can be drawn for the NRZ modulation.

Optics EXPRESS

Special care concerning the optical path difference (OPD) between the channels is required [18,19]. Indeed, to successfully achieve a telecom modulated beam combining, one must properly synchronize the same bit sequence time slot on all combined arms. Thus, the OPD should not exceed a fraction of 19 mm, which is the equivalent length of the bit time in a fiber. By cautious investigation of the length of each fiber component of the two channels using an Optical Backscatter Reflectometer (OBR, 10 µm sampling resolution, 1 mm accuracy); we adjusted the OPD length differences to less than 5 mm using homemade fiber patches, corresponding time delay in fiber of 25 ps.

The output of the 50/50 coupler is divided into the following paths:

- The bottom "LOCSET arm" contains the LOCSET phase controller that maintains destructive interferences on 40 MHz detector and constructive interferences on the top arm used for telecom signal analysis. The EOM tagging frequency (26 MHz) is demodulated on the interfering signal seen by the detector D (40 MHz bandwidth) using numerical synchronous detection. The demodulated signal is the phase error signal that is fed into a PID-controller connected to the EOM to nullify the phase difference [17]. In this case, the controller is configured to lock the phase on destructive interferences instead of usual constructive interferences on detector D 40 MHz. This ensures that the top arm will get the maximum power.

- The top "observation arm" is used to monitor the CBC signal. The combined beam is detected by a photodetector D (30 GHz bandwidth) connected to a 25 GHz bandwidth digital oscilloscope (sampling rate 50 GS/s). Thanks to large electrical bandwidth, we can observe the time evolution of data modulation but also large frequency analysis of CBC in closed or open loop by Fourier Transform of temporal waveform.

- The middle "telecom signal analysis arm" includes a bit error rate (BER) measurement. This arm is composed of a one bit delay interferometer (MZI, placed in the DPSK case only), for a direct detection DPSK receiver [20]; the signal then goes through a variable optical attenuator (VOA) before being detected in a 10 GHz PIN photodiode followed by a transimpedance amplifier (PIN-TIA) for BER assessment.

2.2. *Free space optics configuration (FSO)*

In FSO configuration (Fig. 2), the telecom signal is split by the 1-to-8 fiber splitter. Three outputs are connected to an EOM and a 3W EDFA. The EDFAs output power is limited to 0.2 W for most of the experiments presented in the paper (and up to 3 W at the end of the reported study). The three EDFA outputs are plugged into the original laser head [13], a 27 mm pitch hexagonal array using 100 mm focal length collimation lenses. The tiled pupil total size is about 54 mm for the three channels arrangement. As for the AF setup, we meticulously measured the full fiber paths from the local oscillator to each channel fiber output using the OBR. We have been able to equalize all OPDs using homemade fiber patches with a precision better than 10 mm. In the laboratory environment, we use a 35/500 magnification telescope to reduce the size of the combined beam at pupil output.

A 50/50 beam splitter cube (BS) is used to split the combined beam, one part is sent to a 500 µm pinhole followed by a 40 MHz bandwidth photodetector for far field imaging. The pinhole filters the central lobe of the far field and the LOCSET phase controller maximizes the power on the detector, thus performing CBC operation.

The second part of CBC beam propagates within a 150/500 magnification telescope and a BS cube. It is finally imaged onto an observation camera (640×512 pixels, 15 µm pixel pitch, and 30 Hz frame rate) and simultaneously collected by a 10 µm-core single mode optical fiber, which also plays the role of spatial filtering, rejecting the side lobes.

Finally, the fiber coupled telecom CBC signal is split by a 50/50 coupler towards both the monitoring oscilloscope and the telecom signal analyzer arm, already presented in the previous subsection.

Optics EXPRESS

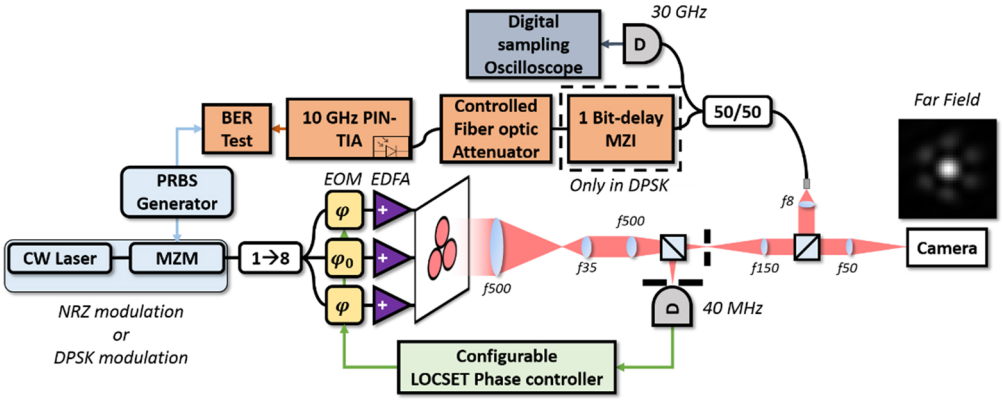

Fig. 2. The FSO Telecom-CBC laser emitter setup. Pseudorandom binary sequence (PRBS) fed to the Mach-Zehnder Modulator (MZM) in order to deliver a DPSK modulated signal. This signal is split towards the three Electro-optical phase modulators (EOM or φ). Each channel is then amplified by an EDFA before being connected to the laser head. Photodiodes (D) is used for phase-locking and signal observation is carried out by a camera and a collecting fiber. Similar layout can be drawn for the NRZ modulation

3. Impact of the telecom signal on the coherent beam combination

3.1. Effect of telecom modulations on the CBC Far-field measurement

First of all, closing the LOCSET phase controller using the same set of parameters with/without an NRZ or DPSK telecom signal results immediately into achieving combination. Figure 3 shows the irradiance distributions of the fringes in FSO configuration. The CBC figure is made of a regular bright and dark fringe pattern (Fourier transform of the fiber array) modulated by a spatial envelope (Fourier transform of one single Gaussian beam) [13,21,22]. The picture (a) displays the lack of interferences when combining channels with mismatched OPD of dozens of times the length of 19 mm (length equivalent to a bit time), because it affects the visibility of the fringes (if the beam powers are equal and stable over time) [18,19] . When OPD is rightly set, one can observe CBC either with 2-channels in picture (b) or 3-channels CBC in picture (c), when the DPSK telecom modulation is active.

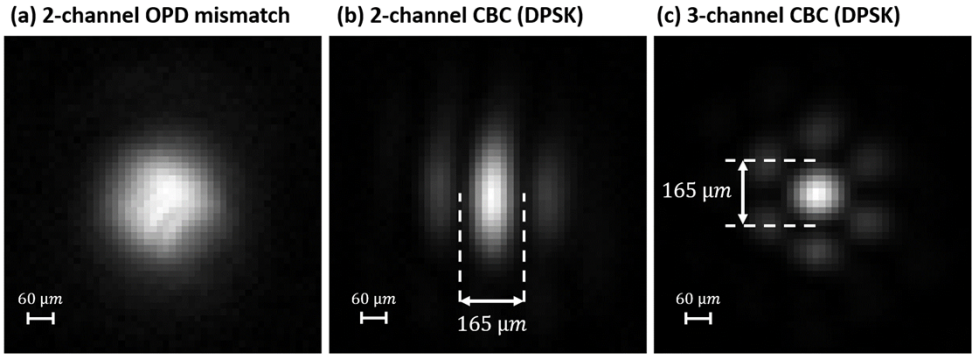

Fig. 3. Far-field irradiance pattern in the case of DPSK modulation with (a) 2-channels CBC with OPD mismatch (b) 2-channels CBC (c) 3-channels CBC.

In the FSO configuration, we use two typical CBC far-field metrics to quantify the quality of the closed-loop combination:

Optics EXPRESS

The first metric is the fringe contrast. In the example shown in Fig. 3(a), OPD is the main factor of fringe contrast drop: the lower the contrast the greater the OPDs between the different laser channels ([18], section 4.2). Otherwise, in general, the drop in contrast may be due to a number of other reasons: power imbalance, spatial overlap, polarization, or phase control instability. In this section, we made sure to keep these parameters stable (almost equal power for the beams, positioning of far-field beams, etc.). The contrast is measured by circling the central lobe, and collecting the average pixel values (mean of 4 pixels) on the peak of the bright fringe in this area and the mean of the dark fringes at midpoint, where the intensity is minimal.

The second metric is the Power-In-the-Bucket (PIB), which is of classical use for beam combination [22]. Here, the relative PIB is the power integrated within the main lobe of the beam, divided by the total integrated power. For 3-channel CBC in hexagonal array, the integration area is a disk circling the main lobe. In that case, the experimental diameter of the main lobe on the camera is $d_{CBC}^{exp} \approx 165\ \mu m$, either in CW, NRZ or DPSK in agreement with a diffraction-limited theoretical size of $d_{CBC}^{th} = 2.44\lambda f/D \approx 166\ \mu m$ (with λ the wavelength, f the focal length of the focus lens on the camera, and D the tiled pupil size accounting for the magnifications) [13,21,22]. For 2-channel CBC, the integration area is a rectangle that outlines the central fringe. Indeed, the linear array made by the two beams has a width of D, but a height of $\leq D/2$, which leads to measure two diffraction-limited dimensions in the far field, roughly d_{CBC}^{th} and $2d_{CBC}^{th}$. The PIB quantifies the effect of transmittance and wavefront aberrations of the whole optical system on the far field. In the laboratory and in open-loop, PIB is mainly dominated by phase variations between combined beams. In closed-loop, it is dominated by high-order wavefront aberrations [23].

We applied these two metrics on 3 different situations: CW, NRZ, DPSK. Results are gathered in Table 1 and Table 2 for 2- and 3-channels CBC respectively.

Table 1. 2-channel CBC far-field metrics results (average values).

Metrics	Classical CW	Telecom NRZ	Telecom DPSK
Fringe contrast (precision of 0.004)	0.928	0.838	0.789
PIB in the main lobe (precision within 1%)	54%	51%	51%

Table 2. 3-channel CBC far-field metrics results (average values).

Metrics	Classical CW	Telecom NRZ	Telecom DPSK
Fringe contrast (precision of 0.002)	0.950	0.926	0.919
PIB in the main lobe (precision within 0.5%)	36%	34.5%	33.1%

Compared to the CW case, the fringe contrast drops slightly either with 2-channels or 3-channels CBC when a telecom modulation is carried by the laser emitter. This confirms that the OPD may be carefully equalized, as stated in section 2, as well as in [18,19]. The PIB measurements follow this same slight decrease, considering the precisions we computed.

3.2. *Effect of telecom modulations on the residual phase*

To complete the far-field measurement, we have investigated residual phase in closed-loop for the 2-channel combination using an optical In-phase and Quadrature (IQ) interferometer (see

Optics EXPRESS

the Fig. 4 for example on FSO configuration). The two fibered photodetectors (100 µm core) are positioned on the interference pattern so that the signals I and Q collected from the fringes are in quadrature. Provided some calibration, the inverse tangent of the quotient provides the phase difference between the two channels, and the residual phase in case of closed-loop. The bandwidth of our IQ interferometer is 2 MHz.

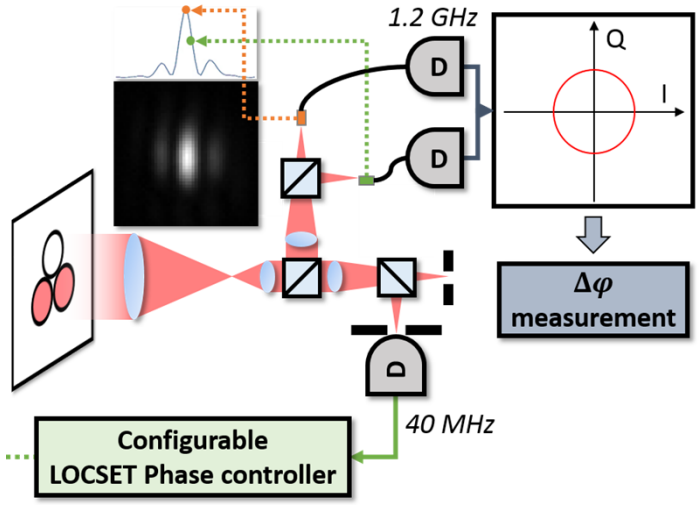

Fig. 4. Additional IQ interferometer installed onto the FSO configuration enabling 2-channels phase measurement. The orange and green fibers have an offset so that the recorded signal are in quadrature (Lissajous curve).

Figure 5 shows the phase power spectral densities (PSDs) of the 2-channel CBC when operated in open-loop (blue curves), and in closed-loop (orange curves) in CW and with NRZ and DPSK modulation. The LOCSET phase controller parameters are optimized in the CW regime and not changed in other regimes. The major contributors of the phase noise come from thermal and mechanical sources in Hz – kHz range and from electronics sources above kHz [24–26]. Those contributors are well corrected by the LOCSET phase controller for all cases below 2 kHz. However, with telecom signal, above 2 kHz, the phase noise in closed loop is higher than in open loop, which exhibits itself more noise than in CW. We attribute this phenomenon to the fact that the LOCSET compensates for some variations coming from the data signal. Indeed the telecom signal presents spectral components at the LOCSET tag frequency leading to an over-modulation of the tag signal that the loop is trying to compensate for. We can also observe that the phase PSD in closed loop is lower in the case of DPSK than in NRZ. This can be explained by the fact that information in the case of DPSK modulation format is carried by the coding of the phase which disappears after quadratic detection in the LOCSET loop.

The residual phase RMS value for each case has been integrated from the power spectral densities. For the CW case, a residual phase (phase-locking quality) of $\lambda/150$ RMS has been achieved; it jumps to $\lambda/60$ RMS in the NRZ case and to $\lambda/125$ RMS in the DPSK case which confirms the above analysis.

As a conclusion on this part, we observe that, for an unchanged set of parameters, the LOCSET CBC is slightly affected by the presence of a telecom amplitude or phase modulation (NRZ or DPSK) but the phase locking is still very efficient as the residual phase remains below $\lambda/60$ RMS. From now on, we will evaluate the quality of the received telecom signal in the presence of the LOCSET loop.

Optics EXPRESS

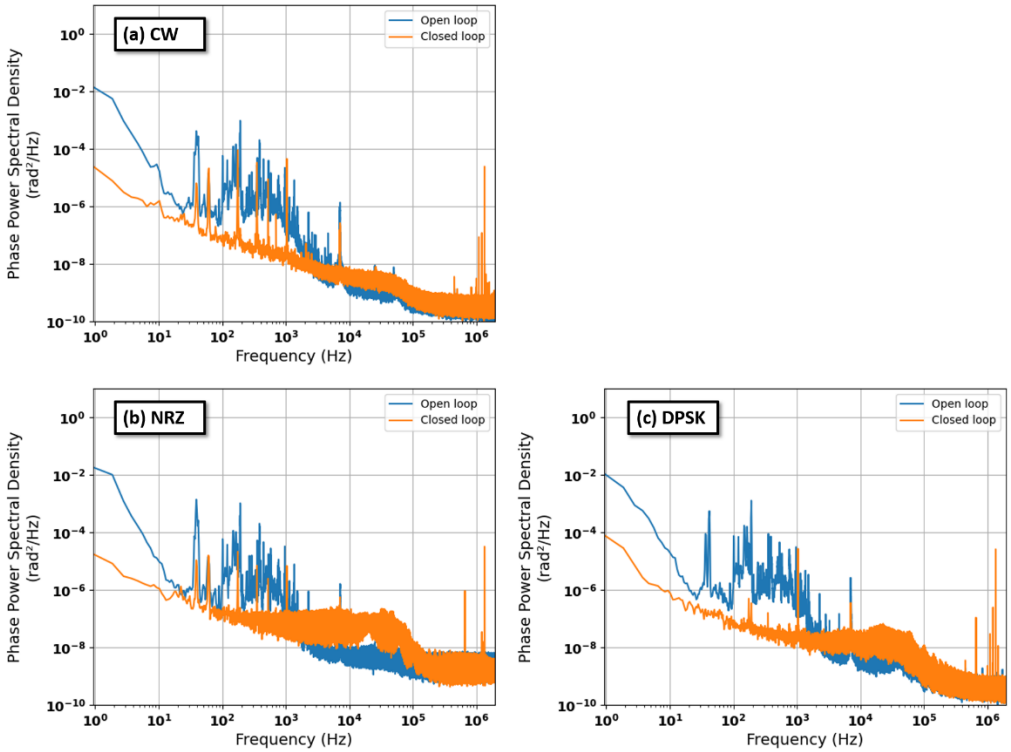

Fig. 5. Power spectral densities of the residual phase for (a) CW-CBC (b) NRZ modulated CBC and (c) DPSK modulated CBC. Data integrated from 10s-long time series. Blue curves: open loops, orange curves: closed loops.

4. Impact of the coherent beam combination on the telecom signal

4.1. Eye-diagram analysis

The CBC modulated signal eye diagram was derived from the waveform measured using a 25 GHz real time digital sampling oscilloscope and a 20 GHz photodiode.

In Fig. 6, the top panels display eye-diagram measurements in NRZ modulation of the reference channel (left) and of the CBC two channels in the AF configuration (right).

In the single channel situation, rise and fall time are around 31% and 32% of the bit time, whereas in the two channels case, rise and fall time increase to 42% and 51% of the bit time; moreover the crossing point is at 48% of the amplitude instead of 50% in the single channel case. We attribute this degradation to the residual OPD. In order to confirm this, we performed numerical simulation. Figure 6 bottom panels display the eye diagrams calculated with one electrical field carrying a 10.66 Gbit/s NRZ signal after quadratic detection with an electrical bandwidth of 20 GHz; the left figure represents a single signal and the right figure represents the detection of the summation of the two electrical fields delayed by 23 ps (corresponding to an OPD of 4.6 mm in the optical fiber). The simulated eye diagram of the 2-channel case is close to the experimental observation confirming the effect of OPD on the temporal eye closure.

Optics EXPRESS

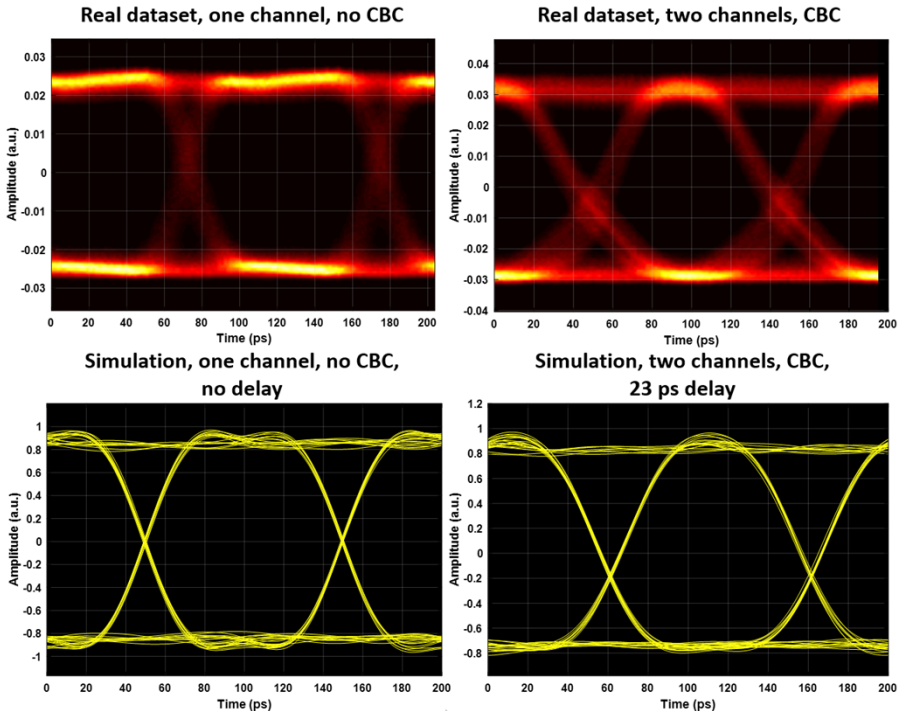

Fig. 6. Eye-diagrams in NRZ modulation for the reference channel alone (upper left) and a two-channels CBC with the all-fiber configuration (upper right). In comparison, simulations were made a posteriori and exhibits similar behavior for both situations, especially for a delay of 23 ps which lies within the error range of our OPD's matching.

4.2. Impact of the LOCSET tagging amplitude on the bit error rate

A key element in CBC is the LOCSET phase controller and BER measurements can be used to investigate its effect on the telecom signal. In order to isolate LOCSET effects from FSO effect, the AF configuration is preferred.

In LOCSET phase controller [17], the phase of each beam carries a low-amplitude RF phase modulation, except for the reference arm. The RF tagging modulation amplitude fed to the EOMs is expressed as a fraction of the modulator's half-wave voltage $V\pi$.

We measured the BER versus average received power for different values of $V/V\pi$ in order to assess its impact. Comparison for a reference measurement and three cases of $V/V\pi$, for both NRZ and DPSK modulations, are displayed in Fig. 7. What emerges directly from these measurements is that there seems to be an optimal range of $V/V\pi$ ratios that minimizes the BER for both modulations. Then, for others values of $V/V\pi$, either too small or too close to 1, the BER rapidly increases, or reaches an error floor. In the case of the finest tunings, a small penalty of 1 dB at 10^{-9} in the NRZ case and 1.5 dB at 10^{-9} in the DPSK one have been measured. Not represented here, similar results were observed in FSO with the combination of two beams (not represented here).

In CBC, tuning the $V/V\pi$ toward 0 is equivalent to operate in open loop (no phase locking). On the other hand, tuning the $V/V\pi$ toward 1 induces too high phase modulation leading to amplitude modulation after beam combination and finally disturbing the telecom signal.

To go further, we will now compare the BER measurements with the LOCSET performance metrics as a function of the tagging modulation amplitude. Figure 8 shows the superimposition

Optics EXPRESS

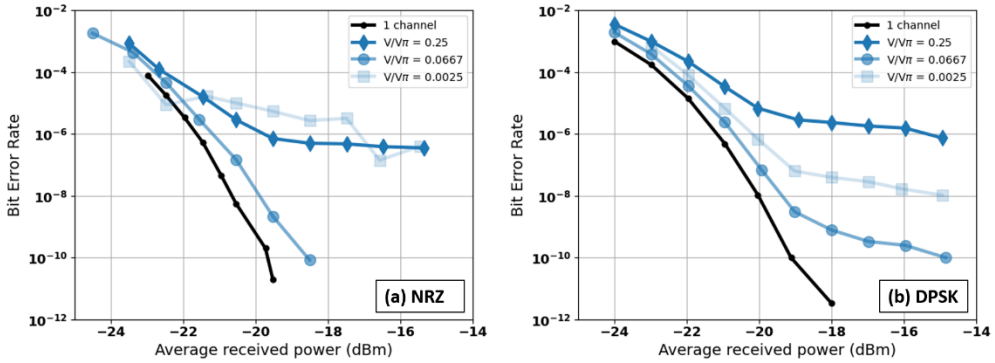

Fig. 7. Bit Error Rate (BER) measurements for both NRZ and DPSK modulations, in the AF configuration (2 channels), in regard to LOCSET modulation depth in V/ Vπ (blue tones). The black curve is our reference. BER is in logarithmic scale.

of the BER at a constant average received power, the residual phase RMS (expressed in terms of λ/N) and the fringe contrast.

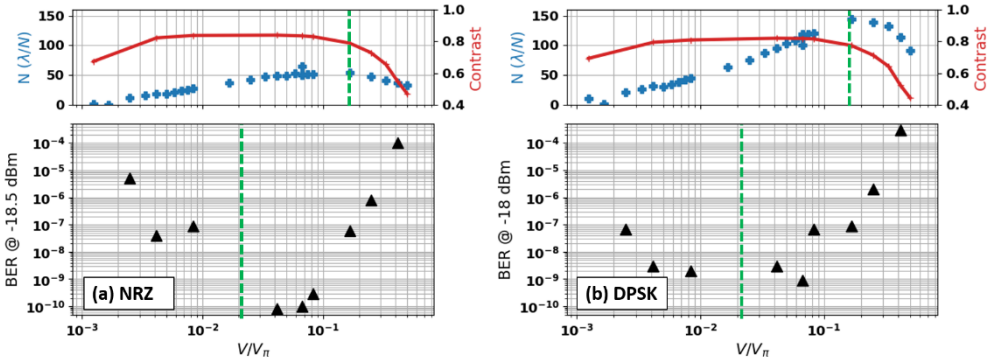

Fig. 8. Comparison between BER (bottom panel), residual phase (in terms of N from λ/N RMS), and contrast (top panel) versus the V/Vπ ratio, modulation depth of the LOCSET phase-loop. In green, dotted lines indicate optimal V/Vπ ratios for both residual phase and BER.

We observe an optimum BER for V/Vπ around 2×10^{-2} whereas the minimum residual phase RMS is obtained for V/Vπ around 1.8×10^{-1}. As presented previously in Fig. 5 (V/Vπ around 1.7×10^{-1}), the phase power spectral density are noisier with telecom signal. However when we increase the tagging amplitude depth, we improve the ratio of the tagging signal amplitude to the telecom signal amplitude at the tagging frequency, which can explain the improvement of the residual phase RMS. But when the tagging amplitude becomes too high, the resulting strong phase modulation after EOM disturbs the beam combining coherence which leads to a decrease of the residual phase RMS and the BER performance. In conclusion, the residual phase RMS measurement is perturbed by the presence of telecom signal and is not a good metric to evaluate the CBC quality in this case.

Consequently we also measured the fringe contrast as a function of the tagging amplitude as depicted on Fig. 8. This time, the maximum fringe contrast is in good agreement with the minimum BER and we believe that the fringes' contrast would be a mandatory information to optimize the tagging amplitude in the presence of telecom signal.

Optics EXPRESS

4.3. Impact of channel number and optical power on the bit error rate

In this section, we study the impact of the number of channels and the EDFA output power in FSO configuration.

4.3.1. Impact of the number of channels

The V/Vπ is tuned to 0.08 corresponding to a good fringe contrast and BER. Residual phase RMS remains < λ/40, which remains a standard value in CBC.

Figure 9 displays the BER for 1, 2 and 3 channels in NRZ and DPSK cases. The 1st observation is that with more than one channel and whatever the modulation format, an error floor is present in the measurement. We attribute this to the residual OPD leading to a time closure of the eye diagram and inter-symbol interferences as explained in paragraph 4.1. With 2 channels, we tested two path combination possibilities with respective OPD of 6 and 10 mm, showing that the higher OPD increases the error floor. The 3 channel case is finally close to the 2 channel case with highest OPD.

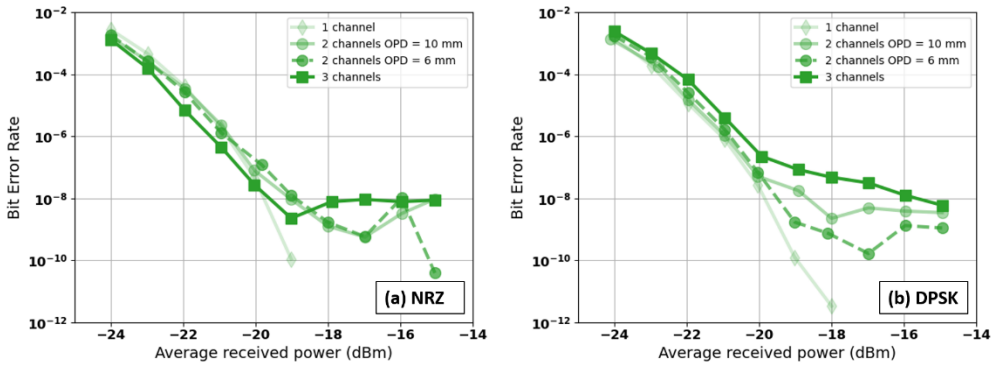

Fig. 9. Bit Error Rate (BER) measurements for both NRZ and DPSK modulations, in FSO configuration, in regard with the number of fiber channels combined in the far-field (green tones). The 2-channels case is made twice combining one with the reference, with each of the two remaining channels having a different OPD (see legend). BER is in logarithmic scale.

4.3.2. Output power of the fiber amplifiers

In this last section, the relative and total power of each channel is studied. Say, a CBC-based telecom laser emitter would be composed of several sub-aperture beams combined altogether. It could happen very occasionally that one of the amplifiers has a failure that reduces its output power. This scenario has been reproduced in our FSO configuration by downscaling the EDFA output power of one channel to 50 mW, while the others remain at 0.2 W. BER measurements are given in Fig. 10 for three cases: no power disparity (all EDFA at 0.2 W), the reference channel (used as a phase reference in the LOCSET phase controller) is decreased to 50 mW and one of the locked channel is decreased to 50 mW. We observe that the change in BER is more impactful if the reference channel encounters a power downgrade. Whenever the situation happens for another channel, the change in BER is less significant and comes down to the 2-channels case as only the attenuated channel is impacted by a poorer locking.

In the last experiment, the power of the fiber array has been increased until it reaches its maximum, i.e. the EDFAs output power will be set to 3 W each. From our previous work on CBC, we know that it will increase the phase noise that has to be compensated for [24–26]. We measured three power level increases of the channels: 0.2 W, 1.5 W then 3 W per EDFA, therefore

Optics EXPRESS

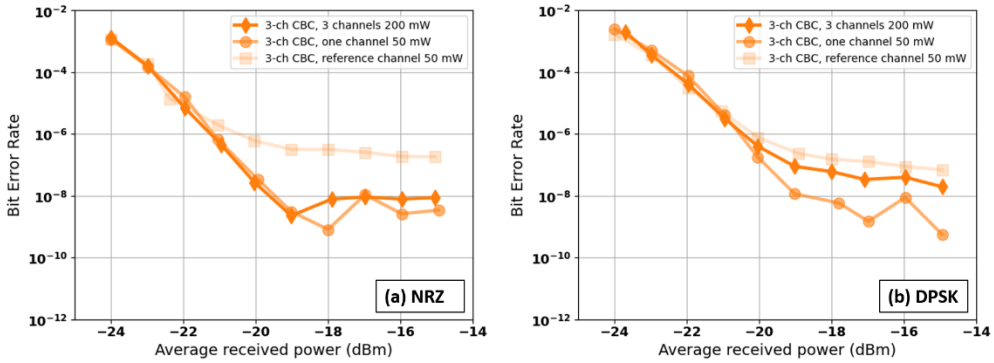

Fig. 10. Bit Error Rate (BER) measurements for both NRZ and DPSK modulations, in FSO configuration, in regard with power disparity (orange tones). BER is in logarithmic scale.

a total of 9 W at the emitter plane. Figure 11 summarizes the results of this last experiment, which shows a good stability of the BER with no significant penalties regardless of the EDFAs power. This last result is an observation of great interest, and opens the way to the development of CBC transmitters with more channels and larger power.

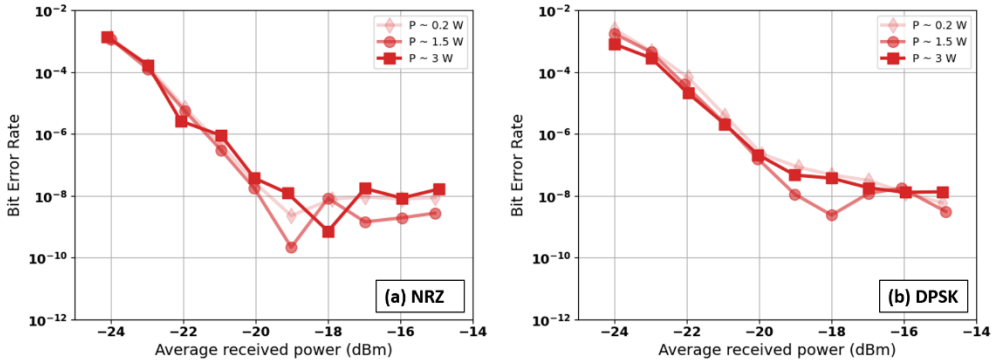

Fig. 11. Bit Error Rate (BER) measurements for both NRZ and DPSK modulations, in FSO configuration, versus power increase of the EDFAs (red tones). BER is in logarithmic scale.

5. Conclusion and perspective

This paper has demonstrated a first experimental demonstration of free-space Coherent Beam Combining (CBC) of amplified NRZ and DPSK telecom signals at 10.66 GHz frequency. The impact of a telecom modulation on the CBC metrics, such as the Power-In-the-Bucket (PIB), fringes contrast, phase noise power spectral densities and residual phases have been studied. Results support that CBC is achievable almost seamlessly, with residual phases of $\lambda/40 \sim \lambda/60$ in NRZ and $\lambda/100 \sim \lambda/150$ in DPSK compared to a CW case presenting a $\lambda/150$ residual phase. For the LOCSET phase controller parameters to be in good adequacy with telecom application, an optimization of phase tagging depth is required of each beam, relative to the Vπ of the phase modulators used. Regardless of the modulation format considered or the number of fiber channels combined, beam combining causes an error floor owing to the residual optical path difference. The study demonstrates that the OPD is a critical issue when carrying data on CBC signal as it will become even more critical at higher bit rate. Power disparity up to 25% has low impact on

Optics EXPRESS

the BER except if the reference untagged beam carries the power downgrade. Finally, an increase of the fiber array power up to 3 W per channel does not increase the BER.

It paves the way to new developments of CBC for the conception of telecom emitter. Especially, future works will likely include active optical path difference (OPD) nulling using delay-lines, such as in femtosecond regime CBC [27], demonstration of a good fit for wavelength-division multiplexing use with CBC, and the exploration of other modulation formats.

Acknowledgments. A. Liméry and F. Gustave from ONERA for help on splicing the fibers and explanations on the operation of the Modbox, as well as the fast oscilloscope. The authors thank the Persyst platform from FOTON Institute (http://persyst.foton.cnrs.fr/) for the setup of the telecom test benches.

Disclosures. The authors declare no conflicts of interest.

Data availability. Data underlying the results presented in this paper are not publicly available but may be obtained from the authors upon reasonable request.

References

1. Y. Arimoto, "Possibility of high-speed optical feeder-link and its demonstration experiment," in *1999 IEEE LEOS Annual Meeting Conference Proceedings* (IEEE, 1999), pp. 45–46, vol.1.
2. P.-D. Arapoglou and N. Girault, "Optical feeder link architectures for very HTS: issues and possibilities," Proc. SPIE **11180**, 201 (2019).
3. R. Saathof, W. Crowcombe, S. Kuiper, N. van der Valk, F. Pettazzi, D. de Lange, P. Kerkhof, M. van Riel, H. de Man, N. Truyens, and I. Ferrario, "Optical satellite communication space terminal technology at TNO," Proc. SPIE **11180**, 19 (2019).
4. Z. Sodnik, C. Voland, J. Perdigues, E. Fischer, K. Kudielka, and R. Czichy, "Optical feeder-link between ESA's optical ground station and Alphasat," Proc. SPIE **11852**, 44 (2020).
5. A. Montmerle Bonnefois, J. -M. Conan, C. Petit, C. B. Lim, V. Michau, S. Meimon, P. Perrault, F. Mendez, B. Fleury, J. Montri, and N. Védrenne, "Adaptive optics pre-compensation for GEO feeder links: the FEEDELIO experiment," Proc. SPIE **11180**, LTh1B.3 (2019).
6. M. Welch, A. Donnot, J. Edmunds, M. Kechagias, E. Prowse, K. Hall, P. Kean, and S. Kehayas, "High power WDM sources for laser communication," Proc. SPIE **11993**, 16 (2022).
7. H. Zhang, M. Bigot-Astruc, L. Bigot, P. Sillard, and J. Fatome, "Multiple modal and wavelength conversion process of a 10-Gbit/s signal in a 6-LP-mode fiber," Opt. Express **27**(11), 15413–15425 (2019).
8. A. Le Kernec, L. Canuet, and A. Maho, *et al.*, "The H2020 VERTIGO project towards tbit/s optical feeder links," Proc. SPIE **11852**, 1185217 (2021).
9. A. Billaud, A. Reeves, A. Orieux, H. Friew, F. Gomez, S. Bernard, T. Michel, D Allioux, J. Poliak, R. Mata Calvo, and O. Pinel, "Turbulence Mitigation via Multi-Plane Light Conversion and Coherent Optical Combination on a 200 m and a 10 km Link," in *2022 IEEE International Conference on Space Optical Systems and Applications* (ICSOS, IEEE, 2022), pp. 85–92.
10. T. Y. Fan, "Laser beam combining for high-power, high-radiance sources," *IEEE Journal of Selected Topics in Quantum Electronics*, **11**(3), pp. 567–577, (2005).
11. M. Müller, C. Aleshire, A. Klenke, E. Haddad, F. Légaré, A. Tünnermann, and J. Limpert, "10.4 kW coherently combined ultrafast fiber laser," Opt. Lett. **45**(11), 3083–3086 (2020).
12. T. Weyrauch, M. A. Vorontsov, G. W. Carhart, L. A. Beresnev, A. P. Rostov, E. E. Polnau, and J. Jiang Liu, "Experimental demonstration of coherent beam combining over a 7 km propagation path," Opt. Lett. **36**(22), 4455–4457 (2011).
13. B. Rouzé, L. Lombard, H. Jacqmin, A. Liméry, A. Durécu, and P. Bourdon, "Coherent beam combination of seven 1.5 µm fiber amplifiers through up to 1 km atmospheric turbulence: near- and far-field experimental analysis," Appl. Opt. **60**(27), 8524–8533 (2021).
14. M. Veinhard, S. Bellanger, L. Daniault, I. Fsaifes, J. Bourderionnet, C. Larat, E. Lallier, A. Brignon, and J.-C. Chanteloup, "Orbital angular momentum beams generation from 61 channels coherent beam combining femtosecond digital laser," Opt. Lett. **46**(1), 25–28 (2021).
15. I. Fsaifes, C.-A. Ranély-Vergé-Dépré, M. Veinhard, S. Bellanger, and J.-C. Chanteloup, "Far field energy distribution control using a coherent beam combining femtosecond digital laser," Opt. Express **31**(5), 8217–8225 (2023).
16. M. Antier, J. Bourderionnet, C. Larat, E. Lallier, E. Lenormand, J. Primot, and A. Brignon, "kHz Closed Loop Interferometric Technique for Coherent Fiber Beam Combining," *IEEE Journal of Selected Topics in Quantum Electronics*, **20**(5), pp. 182–187, (2014).
17. T. M. Shay, V. Benham, J. T. Baker, Benjamin Ward, A. D. Sanchez, M. A. Culpepper, D. Pilkington, J. Spring, D. J. Nelson, and C. A. Lu, "First experimental demonstration of self-synchronous phase locking of an optical array," Opt. Express **14**(25), 12015–12021 (2006).
18. B. Anderson, A. Flores, R. Holten, and I. Dajani, "Comparison of phase modulation schemes for coherently combined fiber amplifiers," Opt. Express **23**(21), 27046–27060 (2015).

Optics EXPRESS

19. G. D. Goodno, S. J. McNaught, J. E. Rothenberg, T. S. McComb, P. A. Thielen, M. G. Wickham, and M. E. Weber, "Active phase and polarization locking of a 1.4 kW fiber amplifier," Opt. Lett. **35**(10), 1542–1544 (2010).
20. G. P. Agrawal, *Fiber-Optic Communication Systems*, 3rd edition, (Wiley-Interscience, 2002), chap.10.6.
21. M. F. Spencer, D. E. Thornton, M. W. Hyde, and J. Bos, "Piston phase compensation of tiled apertures in the presence of turbulence and thermal blooming," *2014 IEEE Aerospace Conference*, (IEEE, 2014), pp. 1–20.
22. M. A. Vorontsov and S. L. Lachinova, "Laser beam projection with adaptive array of fiber collimators. I. Basic considerations for analysis," J. Opt. Soc. Am. A **25**(8), 1949–1959 (2008).
23. B. Kim, N. Jeongkyun, and J. Yoonchan, "Analysis of Power Degradation and Distortion in Coherent-Beam Combining with Lens Aberration," Korean Journal of Optics and Photonics **31**(6), 290 (2020).
24. L. Lombard, G. Canat, A. Durecu, and P. Bourdon, "Coherent beam combining performance in harsh environment," Proc. SPIE **8961**, 896107 (2014).
25. L. Lombard, C. Bellanger, G. Canat, L. Mugnier, F. Cassaing, V. Michau, P. Bourdon, and J. Primot, "Collective synchronization and phase locking of fs fiber amplifiers: requirements and potential solutions," Eur. Phys. J. Spec. Top. **224**(13), 2557–2566 (2015).
26. B. Rouzé, I. Fsaifes, S. Bellanger, M. Veinhard, T. Rousseaux, J. Primot, J.-C. Chanteloup, and C. Bellanger, "Phase noise measurements and diagnoses of a large array of fiber lasers by PISTIL interferometry," Appl. Opt. **61**(27), 7846–7851 (2022).
27. J. Le Dortz, A. Heilmann, M. Antier, J. Bourderionnet, C. Larat, I. Fsaifes, L. Daniault, S. Bellanger, C. Simon Boisson, J.-C. Chanteloup, E. Lallier, and A. Brignon, "Highly scalable femtosecond coherent beam combining demonstrated with 19 fibers," Opt. Lett. **42**(10), 1887–1890 (2017).